Learning to Diagnose Cirrhosis via Combined Liver Capsule and Parenchyma Ultrasound Image Features

Shuo Hong Wang*, Xiang Liu*†, Jingwen Zhao*, Jia Lin Song‡, Jian Quan Zhang‡ and Yan Qiu Chen*
*School of Computer Science, Shanghai Key Laboratory of Intelligent Information Processing,
Fudan University, Shanghai, China Email: {sh_wang, xiangliu09, jingwenzhao13, chenyq}@fudan.edu.cn
†School of Electronic and Electrical Engineering, Shanghai University of Engineering Science, Shanghai, China
‡Department of ultrasound, Changzheng Hospital Affiliated to Second Military Medical University, Shanghai, China
Email: jialin19810818@126.com, Wintersnow9090@sina.com

***Abstract*—This paper proposes a novel cirrhosis diagnosis method using high-frequency ultrasound imaging that is able to not only diagnose cirrhosis, but also determine its stage. We propose combined features extracted from both liver capsule and parenchyma texture to avoid the bias caused by considering only one aspect. The liver capsule is localized using a multi-scale, multi-objective optimization method and indices are proposed to measure the smoothness and continuity of the capsule. The parenchyma texture is modeled with Gaussian mixture model (GMM), and the lesions in the parenchyma are detected by a scale-space defect detection algorithm. The degree of pathological changes of the liver is quantitatively evaluated by 7 features describing morphology of the capsule and lesions in the parenchyma. Then SVM classifiers are trained to classify the samples into different cirrhosis stages. Experiment results demonstrate the effectiveness of the proposed method, which outperforms other 4 state-of-the-art methods and the proposed method that solely uses capsule or parenchyma texture features.**

***Keywords*-Computer-aided cirrhosis diagnosis; Ultrasound image processing; Liver capsule; Parenchyma texture**

I. Introduction

Doctors have been using B-scan ultrasound imaging technique for noninvasive and nonradioactive diagnosis of cirrhosis, a severe oncogenic liver disease that may lead to various complications and high mortality [1], [2]. However, human diagnosis depends on large amount of training and experience. Sometimes, the subtle changes of ultrasound images are difficult even for an experienced clinician to discriminate. Furthermore, misdiagnosis due to subjective factors may lead to serious consequences. Computer-aided quantitative analysis can assist to reduce the influence of subjective factors and improve diagnostic accuracy. Therefore, researchers have been working hard to develop methods to enable computer-aided diagnosis of cirrhosis at early stage for target treatments based on ultrasound images [3], [4].

B-scan ultrasound images present a granular texture [5] that reflects the acoustic characteristics of the tissue. For a normal liver, the parenchyma has homogeneous echotexture, and liver capsule is smooth with even thickness, resulting in uniformly distributed small spots in parenchyma region and fine, smooth capsule in ultrasound images. The progression of cirrhosis will result in damaged parenchyma tissue, fibrosis and formation of pseudolobule. Moreover, liver capsule will become unevenly thickened, producing distinctive echo patterns of liver capsule and parenchyma in ultrasound images. Sample images of normal and cirrhosis livers in different stages are shown in Fig. 1.

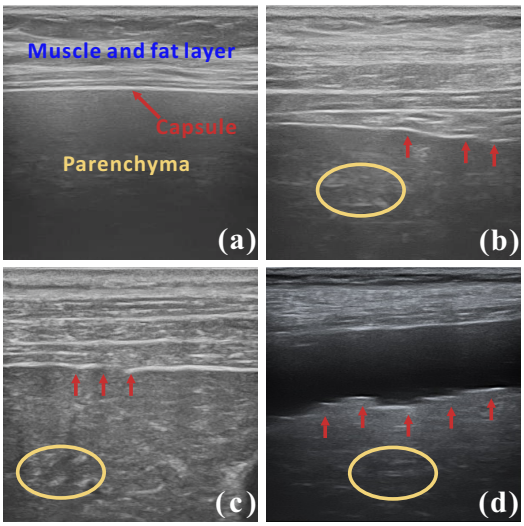

Figure 1: Sample ultrasound images of (a). normal; (b). mild; (c). moderate; (d). severe cirrhosis liver. The red arrows point out the capsule irregularities, the yellow ellipses show the irregular texture of parenchyma, both caused by cirrhosis.

Based on these observations, clinicians and computer-aided diagnosis systems diagnose cirrhosis and determine its progression stages by analyzing the visual features of parenchyma texture and capsule in ultrasound images. Several related works have employed different image analysis techniques to quantitatively analyze the texture of parenchyma in ultrasound images by extracting texture features such as fractal [6], statistical texture [7], or spectral

*Corresponding author: Yan Qiu Chen. This work was supported by National Natural Science Foundation of China, Grant No.61175036.

features [8], *etc*. Then the correspondence between texture features and cirrhosis stages is learned with different classifiers. Combination of several feature extraction methods [4], [9] can make use of the advantages of each method. But as the dimension of feature vector increases, a good feature selection method is vital to guarantee the performance.

In summary, most existing methods focus on analyzing parenchyma texture, therefore investigation of the capsule morphology which is also an important cue for cirrhosis diagnosis is insufficient. Early proposals [3], [10] qualitatively analyze the features of capsule such as diffuse irregularity and thickness which are subject. The diagnostic results are therefore not reliable enough unless it is evaluated together with clinical data. Liu *et al.* [11] used 3 morphological features of capsule alone. Ribeiro *et al.* [12] used features from both capsule and parenchyma. However, their capsule detection method relies on manual initialization. And the extracted capsule cannot reflect its discontinuity caused by cirrhosis. Moreover, as most existing proposals can only determine if the sample is a normal or cirrhosis one, methods that can reliably discriminate the cirrhosis stages is urgently needed to facilitate early diagnosis and target treatments.

To overcome these limitations, the proposed method combines cues from liver capsule and parenchyma texture. Moreover, high frequency ultrasound images are used to improve image spatial resolution, enhance perception of image edges and details and reduce speckle noise [2], making up the shortages of traditional convex array ultrasound probe [10]. The main contributions of the paper lie in:

- Proposing a multi-scale, multi-objective optimization method to extract the liver capsule and 4 indices to characterise the morphology of the capsule;
- Modeling parenchyma texture with Gaussian mixture model (GMM) and localizing lesions in parenchyma by a multi-scale defect detection algorithm;
- Combining cues from liver capsule and parenchyma to accurately and reliably diagnose and discriminate the stages of cirrhosis.

II. Proposed Method

The proposed method combines features from both liver capsule and parenchyma. Liver capsule is first localized using a multi-scale method (Sec. II-A). The texture of parenchyma is modeled with GMM and the nodules in cirrhosis liver are viewed as defects in the image detected by a scale-space method (Sec. II-B). The combined features include the continuity, smoothness of capsule and the statistics of the detected defects in parenchyma. SVMs are then trained to discriminate the stages of cirrhosis (Sec. II-C). The workflow is shown in Fig. 2.

A. Liver capsule analysis

The difference of acoustic impedance between muscle and fat layer and parenchyma forms strong echoes, resulting

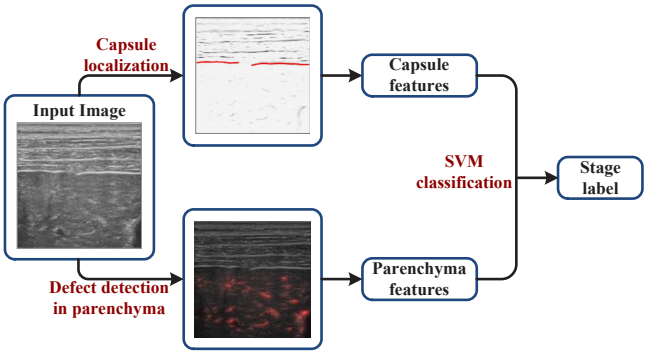

Figure 2: Workflow of the proposed method.

in a bright edge in ultrasound images (see Fig. 1). In the superficial section image obtained by a high frequency probe, normal liver capsule appears as a fine, smooth curve-like structure while the nodular liver surface with diffuse irregularity caused by cirrhosis will result in discontinuous and uneven capsule. Those morphological changes provide an effective way to diagnose cirrhosis by analyzing capsule image features. However, image noises may result in obscure boundary between the capsule and parenchyma and the horizontal textures of upper layer will lead to confusion with the capsule. Moreover, the width and brightness of the capsule vary due to individual differences, and even the ultrasound images taken from the same person may vary a lot. These factors bring about great challenges to existing edge detection methods to reliably localize the liver capsule.

We propose in this paper an automatic method to accomplish the task which first performs multi-scale filtering on the raw ultrasound image, resulting in a capsule enhanced image; then the candidate capsules are extracted by skeleton extraction; lastly, the final capsule is obtained by solving a multi-objective optimization problem.

1) Multiscale image processing: Assume all the scales in scale space consistent with liver capsule is $\mathfrak{S}$. Let one pixel in scale space with scale s be denoted as (x, y, s), the Hessian matrix at the pixel denoted as $\mathcal{H}(x, y, s)$ is calculated by convolution with second order derivatives of Gaussian at scale s. Assume λ_k is the eigenvalue of $\mathcal{H}$ with the kth largest absolute value. $\mathcal{R} = \lambda_1/|\lambda_2|$ reflects eccentricity of the second order ellipse at (x, y), and $\mathcal{S} = \sqrt{\lambda_1^2 + \lambda_2^2}$ reflects the second order structureness. Pixels on the bright, curve-like capsule have negative λ_1 with large $|\mathcal{R}|$ and $\mathcal{S}$. Inspired by [13], we apply $\rho(x, y)$ defined as Eq. (1) to measure the probability that a pixel belongs to a capsule-like structure. One sample result is shown in Fig. 3(b).

$$\rho(x, y) = \max[\rho(x, y, s)], s \in \mathfrak{S}$$
$$\rho(x, y, s) = \begin{cases} 0, & \lambda_1 > 0 \\ 1 - exp[-(\alpha\mathcal{R}^2 + \beta\mathcal{S}^2)], & else \end{cases} \quad (1)$$

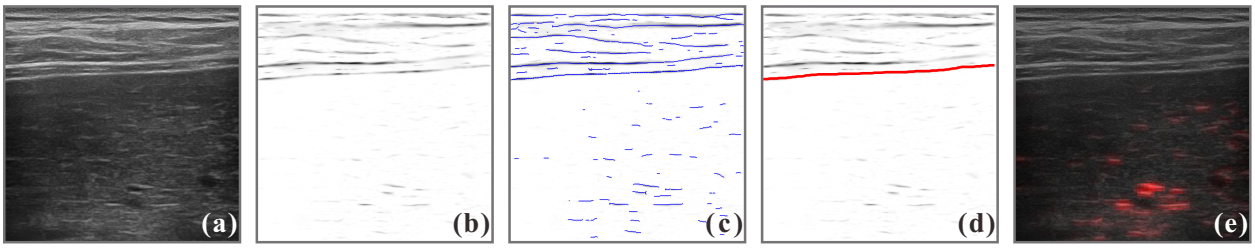

Figure 3: (a). Raw ultrasound image; (b). Resultant ρ of image (a), calculated by Eq. (1), the darkness of each pixel is proportional to the probability that the pixel falls on a capsule-like structure; (c). The candidate capsules (plotted as blue curves); (d). The final capsule (plotted as red curve); (e). Resultant defect map $\mathcal{D}$ of (a), the saturation of red color is proportional to the numeric value of $\mathcal{D}$, which reflects the degree of pathological changes of the nodules in parenchyma.

2) Capsule localization: The next step is to localize the liver capsule based on the capsule enhanced image ρ. Skeleton extraction is first performed on ρ, the resultant candidate capsule curve segments written as $\Gamma_0 = \{C_i \mid i = 1, ..., n_{\Gamma_0}\}$ are plotted as blue curves in Fig. 3(c). Each candidate capsule curve segment consists of n_{C_i} discretized points, $C_i = \{p^j_{C_i} \mid j = 1, ..., n_{C_i}\}$, $p^j_{C_i} = (x^j_{C_i}, y^j_{C_i})$. We select the final capsule curve set based on: 1). liver capsule in high-frequency ultrasound image is the longest curve that separates muscle and fat layer and parenchyma; 2). the horizontal textures that similar with liver capsule are all above the capsule. The resultant capsule curve set is obtained by solving the multi-objective optimization problem in Eq. (2):

$$\begin{aligned} &\tau = \arg\max_{\Lambda} \sum_{i=1}^{n_{\Gamma_0}} \Lambda(C_i)[l_{C_i} \cdot \delta(l_{C_i}),\ \frac{1}{n_\Gamma n_{C_i}} \sum_{j=1}^{n_{C_i}} y_i^j] \\ &s.t. \\ &\Lambda(x) = \{0, 1\}, \quad \bigcap(X_i, X_j) = \varnothing,\ (i \neq j) \\ &\delta(x) = \begin{cases} 0, & x < \varepsilon_l \\ 1, & else \end{cases}, \quad n_\Gamma = \sum_{i=1}^{n_{\Gamma_0}} \Lambda(C_i) \end{aligned} \tag{2}$$

where l_{C_i} is the length of curve segment C_i, X_i is the x coordinate set of capsule curve $\mathcal{C}_i$ in the final capsule curve set $\Gamma = \{\mathcal{C}_i \mid i = 1, ..., n_\Gamma\}$. Candidate curve segment i is in the final liver capsule curve set if $\Lambda(C_i) = 1$. Final capsule curve of Fig. 3(a) is plotted as the red curve in Fig. 3(d).

B. Parenchyma texture analysis

The parenchyma of a normal liver shows homogenous echotexture with medium echogenicity [14] which can be viewed as a random texture with relatively low contrast. With the progression of cirrhosis, the damaged parenchyma tissues will result in uneven intensity distribution and irregular texture caused by the regeneration of nodularity. Doctors diagnose cirrhosis by judging the degree of irregularity in parenchyma echotexture, which depends on the severity of cirrhosis [15]. Inspired by [16], each parenchyma image can be considered as produced by patches of various sizes with random texture (possibly overlapped). A series of representative exemplars functioned as the textural primitives within the normal liver images are modeled with Gaussian mixture model (GMM) and learned by EM algorithm. To localize the lesions caused by cirrhosis which can be viewed as defects in ultrasound images, image patches of different sizes are extracted at each pixel of parenchyma region and tested using the trained exemplars. Test results are then combined to obtain the probability that each pixel is on a lesion.

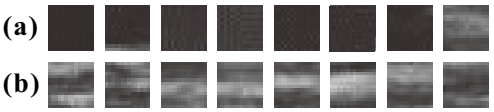

Figure 4: Samples of image patches whose novelty scores are: (a). $< \Lambda^i$; (b). $> \Lambda^i$.

1) Learning multi-scale texems: The texture exemplars (texems) are functioned as the basis of images, which contains the texture primitives. For ultrasound images of normal livers, the textural primitives are consistent. Each texem ϱ_k is characterized by the mean μ and covariance matrix Σ, written as $\varrho_k = (\mu_k, \Sigma_k), k = 1, ..., K$; where K is the number of texems.

The multi-scale strategy enables the texems to represent the spatial interaction of different resolution. The image patches in different scales can be obtained by constructing a Gaussian pyramid and extracting patches from different levels of the pyramid. Assume I^1 represents the parenchyma region in the raw ultrasound image, I^i is the corresponding image at the ith level of the pyramid, then I^{i+1} is calculated by convoluting I^i with Gaussian filter and downsampling. $I^{i+1} = \mathbb{S}^{\downarrow}\mathcal{G}_\sigma(I^i),\ \ i = 1, ..., n_s - 1$. $\mathcal{G}_\sigma$ is the Gaussian convolution, $\mathbb{S}^{\downarrow}$ is the downsampling operation, n_s is the number of levels in the pyramid and $n_s = 4$ in our experiment. Then n_z^i square image patches with size $l \times l$ are sampled from each layer i of the pyramid, written as $Z = \{z_j^i | i = 1, ..., n_s; j = 1, ..., n_z^i\}$. These image patches are firstly reshaped into a vector sized $1 \times l^2$ and grouped by their scales. Thus, an image patch z_j^i corresponds to one point in the space with l^2 dimensions.

If GMM is directly performed in the l^2 dimensional space,

the high dimension will result in too sparsely distributed sample points, making it difficult to model their distribution with GMM. Hence, Principal Component Analysis (PCA) is employed to first reduce the dimension of the samples to d'. We choose $d' = 8$, as according to the experiment results, 8 components explain more than 95% of the total variance. The samples after dimension reduction are denoted as Z'; the probability density function for each patch in Z' is assumed to be subject to Gaussian distribution, written as $p(z'^i_j|\varrho^i_k, \psi^i) = \mathcal{N}(z'^i_j; \mu^i_k, \Sigma^i_k)$, where $\psi^i = \{(\alpha^i_k, \mu^i_k, \Sigma^i_k)|k = 1, ..., K\}, i = 1, ..., n_s$; α^i_k is the prior probability of the kth texem, constrained by $\sum_{k=1}^{K} \alpha^i_k = 1$.

The object is then to obtain the parameter set ψ given the number of texems, which is solved by finding ψ that maximizes the summarized conditional probability over the K texems for all sample image patches:

$$\hat{\psi}^i = = \arg\max_{\psi^i} \sum_{j=1}^{n^i_z} \log(\sum_{k=1}^{K} p(z'^i_j|\varrho^i_k, \psi^i)\alpha^i_k) \tag{3}$$

And the optimization problem is solved by EM algorithm. The novelty score $\mathcal{V}$ defined as Eq. (4) measures the likelihood that patch z'^i_j is generated by texems of level i.

$$\mathcal{V}(z'^i_j|\psi^i) = -\log p(z'^i_j|\psi^i) \tag{4}$$

The lower the $\mathcal{V}$, the more likely the patch belongs to a normal liver. The novelty scores of all the patches z'^i_j extracted from the ith level of Gaussian pyramid correspond to n^i_z points in 1D space. Then K-means clustering is performed on these points to cluster them into r groups. Each cluster is characterized by mean u_r and standard deviation σ_r. As the training samples are extracted from normal liver images, which are viewed as defect-free patches. An upper limit $\Lambda^i = u^i_m + \varsigma\sigma^i_m$ can be set to measure the boundary between good and defective textures of liver image at level i, where cluster m has the maximum mean. According to experiment results, $\varsigma = 5$ best separates the good and defective ones.

2) Lesion localization: For each testing image, a Gaussian pyramid is constructed similar as in the training stage. An image patch with size $l \times l$ is extracted at each pixel of the parenchyma region from each pyramid level. The novelty score of each patch calculated by Eq. (4) reflects the likelihood of defect exists at that pixel at corresponding pyramid level, resulting in a novelty map $\mathcal{V}^i$ with the same size as the parenchyma region of the raw ultrasound image (the four margins are filled by estimated value). Then, the defect map at each level i is computed by comparison of $\mathcal{V}^i$ at each pixel with the upper limit Λ^i, which measures the probability that pixel (x, y) belongs to a defect region.

$$\mathcal{D}^i(x, y) = \begin{cases} 0, & if\ \mathcal{V}^i(x, y) \le \Lambda^i \\ \mathcal{V}^i(x, y) - \Lambda^i, & otherwise \end{cases} \tag{5}$$

in which $\mathcal{V}^i(x, y) \le \Lambda^i$ means that the novelty score at (x, y) from level i is within the up limit of a defect-free patch. Figs. 4(a), 4(b) show the image patches whose novelty scores are less than Λ^i and larger than Λ^i respectively.

Then, $\mathcal{D}^i$ of all levels in the Gaussian pyramid are combined to obtain the final defect map $\mathcal{D}$, indicating the probability that each pixel (x, y) locates on a lesion tissue:

$$\begin{aligned} \mathcal{D}(x, y) &= \frac{1}{n_s - 1} \sum_{i=1}^{n_s - 1} \mathcal{D}^{i,i+1}(x, y) \\ \mathcal{D}^{i,i+1}(x, y) &= \sqrt{\mathcal{D}^i(x, y)\mathcal{D}^{i+1}(x, y)} \end{aligned} \tag{6}$$

The resultant $\mathcal{D}$ of the image in Fig. 3(a) is shown in Fig. 3(e). The saturation of red color is proportional to the value of $\mathcal{D}$, indicating the degree of pathological changes.

C. Cirrhosis diagnosis

The capsule of a normal liver in an ultrasound image has a smooth, hyperechoic straight structure. As the progression of cirrhosis, the regeneration of nodularity will result in wavy, jagged, or stepped changes of capsule and heterogeneous parenchyma texture. Considering these characteristics, 2 continuity and 2 smoothness indices are proposed to evaluate the variation of liver capsule, and another 3 indices to characterize the parenchyma texture.

1) Liver capsule features:

- I. Continuity of liver capsule
  The first index is the percentage of effective length of the capsule, denoted as ζ. Assume the total effective length of all curve segments of a capsule is calculated as:

$$L = \sum_{i=1}^{n_\Gamma} len(\mathcal{C}_i)\delta(i) \tag{7}$$

  where $len(\cdot)$ is the length of each curve segment, $\delta(\cdot)$ is an indicator function, $\delta(i) = 0$ if the curve segment i is shorter than ε_l, otherwise $\delta(i) = 1$, meaning that the curve segments shorter than ε_l are omitted because they often come from the interval between interrupted curve segments. At last, the continuity index ζ is calculated by $\zeta = L/W$, where W is the width of raw ultrasound image. The other index is the number of capsule curve segments n_Γ, defined in Sec. II-A2.
- II. Smoothness of liver capsule
  Each curve segment $\mathcal{C}_i$ of a capsule is discretized into n_{d_i} line segments with equal length, n_{d_i} is proportional to the length of $\mathcal{C}_i$. Then 2 indices are calculated to measure the smoothness of the capsule.
  The one is the average deflection angles θ between adjacent segments, denoted as Θ, and calculated as

$$\Theta = \frac{1}{n_\Gamma} \sum_{i=1}^{n_\Gamma} \frac{1}{n_{d_i} - 1} (\sum_{j=1}^{n_{d_i} - 1} \theta^j_i) \tag{8}$$

  The other is the average variance of the capsule in the vertical direction, denoted as κ given by Eq. (9), where $\mathcal{L}$

is the fitted line based on the resultant capsule points $p_{\mathcal{C}_i}$, $d(\cdot)$ is the distance from point $p^j_{\mathcal{C}_i}$ to line $\mathcal{L}$.

$$\kappa = \frac{1}{n_\Gamma}\sum_{i=1}^{n_\Gamma}[\frac{1}{n_{\mathcal{C}_i}}\sum_{j=1}^{n_{\mathcal{C}_i}} d(p^j_{\mathcal{C}_i}, \mathcal{L})] \tag{9}$$

2) Parenchyma features: Cirrhosis stages are also characterized by the degree of irregularity of parenchyma texture. After lesion localization (described in Sec. II-B), the defect map $\mathcal{D}$ is obtained. The value of each pixel in $\mathcal{D}$ is proportional to the probability that the pixel locates on a lesion. The irregularity of the texture is quantitatively evaluated by the quantity and degree of variation of the lesions. The quantity of lesions is measured by the number of local maxima on unit area of $\mathcal{D}$, denoted as $\chi(\mathcal{D})$. The degree of variation is measured by the mean and entropy of $\mathcal{D}$, denoted as $mean(\mathcal{D})$ and $\mathcal{E}(\mathcal{D})$ respectively. The larger the three metrics are, the more severe the cirrhosis is.

3) Learning to classify: After obtaining the features of liver capsule and parenchyma, a classifier capable of accurately classifying the samples into normal, mild or moderate cirrhosis is vital. Support vector machine (SVM) has shown good performance in nonlinear classification problems with small training set and high dimension as it is less prone to overfitting [17]. SVM accomplishes the classification task by constructing an optimum hyper plane in the high dimensional feature space and separating the samples with minimum expected risk. According to these considerations, SVM classifier is chosen for the proposed method.

Before using SVM, the extracted features are first normalized to $[0, 1]$ to avoid bias caused by unbalanced feature values. Then one-against-one strategy [18] is employed to classify the samples into 4 classes by learning 6 SVMs.

III. Experiments

A. Experiment setup

We used a high-frequency ultrasound probe to obtain 68 subjects' superficial section images. Subjects with cirrhosis at different stages and without cirrhosis were randomly selected under the premise of no significant differences in age, gender and weight. According to Child-Pugh standard, cirrhosis stages are defined as: Level A (mild), Level B (moderate), and Level C (severe). The groundtruth diagnosis results are based on ultrasound, CT and further confirmed by laboratory examination. The cases complicated with other organic liver diseases were not taken into consideration.

The proposed method is implemented with MATLAB$^{\mathrm{TM}}$. In capsule analysis, the scale space $\mathfrak{S}$ is dependent on the range of capsules thickness. We choose $\mathfrak{S} = 0.5t, t = 1, 2, ..., 20$. And the parameters in Eq. (1) are set as $\alpha = 0.6$, $\beta = 0.4$, which achieve the best performance. In parenchyma texture analysis, there are 4 levels in the Gaussian pyramid introduced in Sec. II-B1. Totally 5 ultrasound images of normal liver are chosen and 100 image patches with size 15×15 are randomly extracted from each layer of each image for training. The Gaussian filter for pyramid construction has size 3×3, $\sigma = 0.5$. Then the image patches are reshaped as 1×225 and reduced to 1×8 using PCA.

B. Results and discussions

To evaluate the accuracy of the proposed capsule localization method, the liver capsule of all the 68 sample images were manually marked as groundtruth by an experienced doctor. If the Euclidean distance between one point in computed capsule point set and the groundtruth capsule is less than a threshold ε_e, then the point is judged as correctly located, and we choose $\varepsilon_e = 5\,pixels$. The accuracy of capsule localization for each cirrhosis stage is defined as the percentage of capsule points that are correctly located. The results are shown in Table I. The proposed method achieved higher accuracy on normal liver images than others, as the capsules in images of normal livers are clearer and smoother.

Performance evaluation of the proposed method is based on classification accuracy using a K-fold cross-validation strategy where $K = 5$. The evaluation was performed 100 times on the data set to test the average performance.

Table II shows the classification accuracy of the compared methods. Kalyan *et al.* [7] employed ANN classifier based on GLRLM features. Virmani *et al.* [19] applied Gabor wavelet transform to obtain parenchyma texture features. Lee *et al.* [9] extracted fractal features based on M-band wavelet transform combined with features extracted by spatial gray-level dependence matrices (SGLDM) and dyadic Gabor filter bank. Ribeiro *et al.*'s method [12] uses features from both capsule and parenchyma. These four methods use different kinds of features and obtained high classification accuracy on their data sets. The proposed parenchyma features are obtained by a novel idea of modeling parenchyma texture, we found that combining texture features in other proposals into our method doesn't obviously improve the performance. So, we solely use the proposed texture features to model the degree of pathological changes in parenchyma and combine them with the proposed capsule features.

According to the results in Table II, the proposed method outperforms others on both diagnosing cirrhosis and determining its progression stages. The average accuracy is higher and the standard deviation is lower. That is to say, the proposed method has more stable performance as it combines the features of both capsule and parenchyma, which avoids the bias caused by considering only one aspect

Table I: Capsule localization accuracy on different stages.

Cirrhosis stage	Cases	Accuracy (%)
Normal	20	100.00
Mild	18	98.33
Moderate	17	98.02
Severe	13	97.75

Table II: Classification accuracy evaluation (%)

Method	Normal	Stages of Cirrhosis		
		Mild	Moderate	Severe
Lee *et al.*	79.06±0.09	73.36±0.15	74.49±0.13	73.33±0.15
Kalyan *et al.*	90.12±0.09	76.30±0.13	75.03±0.13	80.06±0.13
Virmani *et al.*	74.39±0.11	77.32±0.13	73.66±0.14	78.81±0.15
Ribeiro *et al.*	84.07±0.09	71.76±0.10	75.19±0.11	89.31±0.10
Proposed	92.46±0.08	80.49±0.06	83.93±0.09	91.98±0.09
Proposed$^{\#}$	89.22±0.09	72.21±0.13	79.35±0.13	91.77±0.10
Proposed*	80.15±0.10	74.45±0.11	82.63±0.07	78.90±0.08

Proposed$^{\#}$ and Proposed* correspond to the proposed method that solely uses capsule features and parenchyma texture features respectively.

Table III: Confusion matrix of the proposed method

		Predicted stage			
		Normal	Mild	Moderate	Severe
True stage	Normal	368 92.46%	24 6.03%	6 1.51%	0 0.00%
	Mild	21 5.77%	293 80.49%	49 13.46%	1 0.27%
	Moderate	5 1.49%	40 11.90%	282 83.93%	9 2.68%
	Severe	7 2.67%	9 3.44%	5 1.91%	241 91.98%

and thus significantly improves the diagnosis accuracy.

We further calculate the confusion matrix using the proposed method. The results in Table III indicate that more misclassification occurs between mild and moderate stages caused by the minor variation of capsule and parenchyma between these two stages. Therefore, more works that concentrate on separating the two stages should be done.

IV. Conclusion

We have proposed in this paper a novel cirrhosis diagnosis method using high-frequency ultrasound imaging. The proposed method combines cues from both liver capsule and parenchyma to avoid the bias of considering only one aspect. The liver capsule is localized using a multi-scale, multi-objective optimization method. The texture of liver parenchyma is modeled with GMM, and the lesions in parenchyma are detected by a scale-space defect detection algorithm. Then 7 features are extracted and SVM classifiers are trained to classify the samples into different cirrhosis stages using one-against-one strategy. Experiments on a data set with 68 samples confirmed the validity of the proposed method. It can be implemented in computer-aided diagnosis systems to assist medical diagnostics.

References

[1] D. Schuppan and N. H. Afdhal, "Liver cirrhosis," *Lancet*, vol. 371, no. 9615, pp. 838–851, 2008.

[2] N. Goyal, N. Jain, V. Rachapalli, D. L. Cochlin *et al.*, "Non-invasive evaluation of liver cirrhosis using ultrasound," *Clin. Radiol.*, vol. 64, no. 11, pp. 1056–1066, 2009.

[3] A. Di Lelio, C. Cestari, A. Lomazzi, and L. Beretta, "Cirrhosis: diagnosis with sonographic study of the liver surface." *Radiology*, vol. 172, no. 2, pp. 389–392, 1989.

[4] C.-M. Wu, Y.-C. Chen, and K.-S. Hsieh, "Texture features for classification of ultrasonic liver images," *IEEE Trans. Med. Imaging*, vol. 11, no. 2, pp. 141–152, 1992.

[5] M. F. Insana, R. F. Wagner, B. S. Garra, D. G. Brown *et al.*, "Analysis of ultrasound image texture via generalized rician statistics," *Opt. Eng.*, vol. 25, no. 6, pp. 256 743–256 743, 1986.

[6] W.-L. Lee and K.-S. Hsieh, "A robust algorithm for the fractal dimension of images and its applications to the classification of natural images and ultrasonic liver images," *Signal Process.*, vol. 90, no. 6, pp. 1894–1904, 2010.

[7] K. Kalyan, B. Jakhia, R. D. Lele, M. Joshi *et al.*, "Artificial neural network application in the diagnosis of disease conditions with liver ultrasound images," *Advances in bioinformatics*, vol. 2014.

[8] A. Mojsilović, M. Popović, S. Marković, and M. Krstić, "Characterization of visually similar diffuse diseases from b-scan liver images using nonseparable wavelet transform," *IEEE Trans. Med. Imaging*, vol. 17, no. 4, pp. 541–549, 1998.

[9] W.-L. Lee, Y.-C. Chen, and K.-S. Hsieh, "Ultrasonic liver tissues classification by fractal feature vector based on m-band wavelet transform," *IEEE Trans. Med. Imaging*, vol. 22, no. 3, pp. 382–392, 2003.

[10] H. Ferral, R. Male, M. Cardiel, L. Munoz *et al.*, "Cirrhosis: diagnosis by liver surface analysis with high-frequency ultrasound," *Gastrointestinal radiology*, vol. 17, no. 1, pp. 74–78, 1992.

[11] X. Liu, J. L. Song, J. W. Zhao, Y. Q. Chen *et al.*, "Extracting and describing liver capsule contour in high-frequency ultrasound image for early hbv cirrhosis diagnosis," in *ICME*. IEEE, July 2016, pp. 1–6.

[12] R. Ribeiro, R. T. Marinho, J. Suri, and J. M. Sanches, "Ultrasound liver surface and textural characterization for the detection of liver cirrhosis," in *Abdomen and Thoracic Imaging*. Springer, 2014, pp. 145–168.

[13] A. F. Frangi, W. J. Niessen, K. L. Vincken, and M. A. Viergever, "Multiscale vessel enhancement filtering," in *MICCAI*. Springer, 1998, pp. 130–137.

[14] J.-W. Jeong, S. Lee, J. W. Lee, D.-S. Yoo *et al.*, "The echotextural characteristics for the diagnosis of the liver cirrhosis using the sonographic images," in *EMBS*. IEEE, 2007, pp. 1343–1345.

[15] E. Caturelli, L. Castellano, S. Fusilli, B. Palmentieri *et al.*, "Coarse nodular us pattern in hepatic cirrhosis: Risk for hepatocellular carcinoma 1," *Radiology*, vol. 226, no. 3, pp. 691–697, 2003.

[16] X. Xie and M. Mirmehdi, "Texems: Texture exemplars for defect detection on random textured surfaces," *IEEE Trans. Pattern Anal. Mach. Intell.*, vol. 29, no. 8, pp. 1454–1464, 2007.

[17] C. J. C. Burges, "A tutorial on support vector machines for pattern recognition," *Data Min. Knowl. Discov.*, vol. 2, no. 2, pp. 121–167, 1998.

[18] A. J. Smola and B. Schölkopf, "A tutorial on support vector regression," *Stat. Comput.*, vol. 14, no. 3, pp. 199–222, 2004.

[19] J. Virmani, V. Kumar, N. Kalra, and N. Khandelwal, "Prediction of liver cirrhosis based on multiresolution texture descriptors from b-mode ultrasound," *International Journal of Convergence Computing*, vol. 1, no. 1, pp. 19–37, 2013.